

Article

Pulse Wave Harmony: Ancient Wisdoms for Modern Age

Patrick Celka ^{1*}, Lobsang Samten ², Marina Brucet ² and Abdullah Alabdulgader ³

¹ SATHeart SA, Yverdon-les-Bains, Switzerland; patrick.celka@satheart.com

² Lama Tzong Khapa Institute, Pomaia, Italy; mbrucet@gmail.com

³ Director of Research and Scientific Bio-Computing, Prince Sultan Cardiac Center, Alhasa, Hofuf 31982, Saudi Arabia; kidsecho@yahoo.com

* Correspondence: patrick.celka@satheart.com

Abstract: Background: This research presents the use of photoplethsmography combined with Traditional Tibetan Pulse reading for the estimation of the three energies of a person: Activity, Transformation and Stability. The growing interest to revive traditional finger pulse reading attests of the need to find alternative ways to approach complex multi-source diseases as well as individualised diagnostic wearable or portable cost effective systems. Method: Our work is presented in two studies. The first study presents the development of the technique of photoplethsmography to classify the three energies. The second study presents a validation of this methodology on mental stress and relaxation. Results: Energies classification achieved a sensitivity above 85% and specificity above 72%. Mental stress and relaxation could be significantly discriminated from baseline condition. Harmonic analysis gave further insights into the dynamic of the pulse wave under stress/relaxation. Conclusion: The photoplethsmogram contains information pertaining to the mental and physiological state of a person as interpreted with the Eastern energies concepts. The implication of this work points towards a holistic understanding and impact of human activities, health and its environment.

Keywords: Pulse wave analysis; Traditional Tibetan Medicine; Harmonic analysis; Mental stress; Holism; Environment

1. Introduction

Western medical practice and science has progressed rapidly since 100 years to reach unprecedented accuracy in diagnostic instruments and surgical practices. Intelligent robots are helping surgeons to perform faster and better operations. Medical data are analysed by artificial intelligent algorithms and help physicians to take better decisions regarding therapeutic treatments. We however see a resurgence of complementary and so-called alternative medicine, including ancient traditional medicinal systems. Indeed the price to pay for a sophisticated instrumented diagnostic arsenal, is the loss of a holistic view on the patient's problems. Traditional medicine systems offer a natural way to counterbalance the analytical approach with a synthetic one. Chronic multiple-sources illnesses such as cancer, multiple-sclerosis and fibromyalgia or even hypertension are less well treated and sometimes diagnosed by Western medicine. One common cause of these diseases originate in stress. Stress can have multiple origins such as internal and external to our body as well as mental. Mental stress is particularly interesting to study in our epoch as it is a common health issue, associated with increased cardiovascular mortality and morbidity [1]. It also has a great impact on both professional and private lives as it has been associated with negative mood [2], immunosuppression [3], impacts on physical and mental health and increased occurrence of illnesses [4].

32 Methods to assess mental stress have been primarily focused on questionnaires. More objective
 33 techniques have emerged based on neurophysiological sensors such as electroencephalogram
 34 and heart inter-beat intervals analysis. Among the most popular sensors are those based on
 35 photoplethysmography (PPG) [5,6] due to their low cost and relative ease of use. The PPG signal is a
 36 surrogate of the blood pulse pressure wave which contains information about the neuro-cardio-vascular
 37 system [7–9] thus offering a potential powerful tool to assess mental stress as manifested in
 38 neuro-physiological responses. Mental stress has indeed been quantified using PPG analysis [10–15].

39 Pulse wave reading has a long history in both Western and Eastern medicinal systems and offers
 40 a powerful diagnostic method. It is thus a legitimate question to ask if traditional pulse reading
 41 methods can be linked to modern pulse wave sensing and processing techniques. As Eastern empirical
 42 medicinal knowledge are slowly transformed into evidence based medicine, Eastern pulse reading
 43 method is indeed currently under rapid modernization using digital techniques [16–23].

44 In this work, we present for the first time a method based on PPG analysis to interpret some
 45 aspects of Traditional Tibetan pulse reading. This method is further used in a mental stress laboratory
 46 experiment. The concepts of traditional pulse reading are verified and analysed in terms of Western
 47 medicine concepts. Additional insights into the use of pulse wave harmonic analysis is presented and
 48 discussed in correlation with time domain pulse wave analysis.

49 The paper is organized as follows. Section 2 presents the basic understanding of Eastern
 50 philosophy together with Traditional Tibetan Medicine concepts and their relationship with Western
 51 concepts. Section 3 describes our two separate data collection protocols and pulse wave sensing
 52 instruments. The first study is presented in Section 4.1 and describes the classification of the three
 53 energies. The second study is presented in Section 4.2 and validate our energies classification together
 54 with a harmonic analysis in the assessment of mental stress. The two studies were independently
 55 performed. Section 5 discusses the results and Section 6 concludes this work.

56 2. Eastern and Western Pulse Reading

57 2.1. Traditional Tibetan Pulse Reading: The Three Energies

58 *Sowa Rigpa*, the Traditional Tibetan Medicine [24] is essentially based on medical texts originating
 59 from Central Asia and Tibet [25] and derives from a collection of texts known as the Four Tantras [26].
 60 The two major contribution to the Traditional Tibetan Medicine came from India [27] and China [28,29].
 61 We can thus say that Traditional Tibetan Medicine is an integration of local Tibetan healing knowledge
 62 with Ayurveda and Chinese medicine.

63 At the core of ancient medical and cosmological knowledge, both from Western and Eastern
 64 cultures, stands the philosophy of the elements [27]. These elements were thought to pervade all of
 65 animate and inanimate objects, perceivable and not. The elements are commonly known as Air/Wind,
 66 Fire, Water and Earth. The elements are not to be conceived as static building blocks but rather as
 67 functional entities or elemental energies that reflect their stability, and their dynamic and transformative
 68 nature. The concept of energy is central in both Western and Eastern sciences and is thus a good base
 69 for making the bridge between the two systems. In order to ease the way from Western to Eastern
 70 thoughts when reading this article, we should keep in mind the following definition of energy: a
 71 measure of a system's ability to cause change or maintain its structure.

72 When concerned with our body, the elements are further reduced to the three energies known as:
 73 Wind (*Lung*), Bile (*Tripa*) and Phlegm (*Beken*). In order to make the bridge with Western concepts easier,
 74 we have tentatively introduced a new terminology. It has to be noticed however that to grasp the full
 75 concept and meaning of these energies in their original context, one should consult specialized books
 76 or have a clear explanation from a Tibetan doctor.

- 77 • Phlegm (*Beken*) = Earth + Water = **Stability**
- 78 • Wind (*Lung*) = Wind = **Activity**
- 79 • Bile (*Tripa*) = Fire = **Transformation**

80 **Stability** is associated with foundational structure. Thus, it is linked with bone and marrow,
 81 flesh and liquids on the body side, and mental quality of calmness and focus. **Activity** is linked
 82 to movements. It can be the nervous system activity, blood flow, physical movement as well as
 83 movements of thoughts and emotions. **Transformation** is linked with heat and clarity. Thus it is linked
 84 with metabolic processes as well as sense perception and mental clarity.

85 Each person possesses a specific *typology* from birth, that is to say a certain proportion of these three
 86 energies. These energies slowly evolves with time and ageing depending on external (environment)
 87 and internal (physiology and mind) conditions. For example, these energies manifest differently in
 88 our body functions according to the four seasons, sun and moon activities (i.e. night and day). They
 89 also varies according to our breathing pattern, cardiovascular condition and cell level functional states.
 90 Pathologies reflect the fact that the three energies at a certain time are in a state of imbalance with
 91 respect to the typology of the person. Thus, the typology is the reference point for the doctor, from
 92 which any departure represents a state of imbalance. A few examples of imbalance are discussed
 93 below. Usually, a mix of these condition appears as the energies are dependent on each other.

- 94 • Elevated **Stability** energy result in obesity due to inactivity, dullness of mind or depression, flu
 95 and immune system dysfunction,
- 96 • Elevated **Activity** energy can manifest as anxiety, mental and physical hyperactivity, hearing
 97 problems, dysautonomia, constipation, or breathing disorders,
- 98 • Elevated **Transformation** energy tends to increase excitability, over joyful state or anger, tendency
 99 towards hypertension and cardiovascular problems.

100 The typology is the natural condition of the person and has to be determined in precise conditions
 101 [24]. To each organ corresponds a predominance of an element and is thus also correlated with a
 102 typology. There is a correspondence between the three energies and physiological, psychological,
 103 energy functions and the senses/sense organs. These correspondences are helpful to cross the bridge
 104 between Eastern and Western way of thinking and their essential correspondences are shown in Table
 105 1.

Table 1. The Three Energies and their Western Correspondences

	<i>Activity (Lung)</i>	<i>Transformation (Tripa)</i>	<i>Stability (Beken)</i>
<i>Physiology</i>	Nervous system, Blood circulation, Lymphatic circulation, Tissue growth, Reproduction, Excretion	Digestion, Skin coloring	Immune system, Bone structure, Joint lubrication
<i>Psychology</i>	Cognition, Anxiety, Distress, Fear, Instability	Creativity, Intuition, Desire, Anger, Joy, Impulsiveness, Extraversion	Tolerance, Generosity, Tranquility, Introversion, Sensation, Feeling
<i>Sense/Organ</i>	Touch (Skin), Hearing (Ears)	Vision (Eyes)	Taste (Tongue), Smell (Nose)
<i>Energy</i>	Movement, Creation, Birth, Aging, Death	Transformation, Discrimination	Structure, Stability, Construction/Cohesion
<i>Pulse</i>	Rough, quick, empty, floating with intermittent beats	Sharp, rolling, strong, fast, overflowing with taut beats	Sunken, slow with very weak beats
<i>Elements</i>	Wind	Fire	Water and Earth

106 The exceptional discovery by ancient physicians that the pulse wave characteristics can be mapped
 107 to the three energies led to great progresses in the art of diagnosis. Pulse reading is one diagnosis
 108 method among others such as urine, tongue or eyes analysis, but pulse diagnosis is the preferred
 109 technique. Tibetan Medicine qualifies the pulse wave using a descriptive method with lots of analogies
 110 of animal features and behaviors [24]. Certain qualities of the pulse are more prominent at certain
 111 locations of the bodies: radial artery at the wrist, carotid artery, forehead arteries (especially at the
 112 temporal sites), ankle arteries (such as lateral tarsal artery). In most cases, the radial artery is used
 113 by the doctor. The traditional doctor position three fingers (index, middle and ring) alongside the
 114 artery on each wrist to perform the diagnosis [30] using various pressure levels on the fingers. Figure 2
 115 illustrates the finger position. This technique involved a physical contact between the patient and the
 116 doctor whereby the doctor uses his respiration when analysing the patient's pulse. The main challenge
 117 that took us about ten years was to translate the Eastern concepts to something that could be used
 118 using modern pulse sensing such as PPG. The Section 2.2 describes such a translation.

119 2.2. Western Pulse Wave Analysis: The Three Principles

120 It is nowadays well known from digital pulse wave analysis that the pulse waveform varies
 121 depending on the body location and contains information about the organs and tissues 'visited' by the
 122 travelling wave from the heart to the periphery [31,32]. Additionally, research started to appear on
 123 the effect of mental processes and emotions using features contained in the pulse wave [10,11,33,34]
 124 which correlates with the Tibetan Medicine approach shown in Table 1. The pulse wave description of
 125 Table 1 can be explained according to the following three principles: **Rhythm** (Quick, slow, fast, rolling,
 126 intermittent, (in)coherent), **Force** (Sunken, strong, empty, weak) and **Complexity** (Rough, sharp).
 127 These three principles can be interpreted using signal processing terminologies with the following
 128 physiological interpretation:

- 129 • **Rhythm**: is the way the heart beat intervals are distributed, fast or slow and regular or irregular,
 130 mainly as a manifestation of the autonomic nervous system activity. This quality can be
 131 reasonably well described using *heart rate*, *heart rate variability* and *breathing frequency* analysis
 132 [35–37],
- 133 • **Force**: is the strength of the blood pressure felt under the fingers. Our PPG sensor capture the
 134 changes in blood oxygenated red cell volumes. These changes are also correlated with increased
 135 diameter at the systole and reduced diameter at diastole. The peak-to-peak *amplitude* of the PPG
 136 signal is thus an indirect measure of the blood pressure [38]. The modulation depth is also felt
 137 under the finger as a varying force. This modulation depth can be measured using well known
 138 techniques of signal modulation for example as used when measuring the periodic breathing in
 139 cardiac patients [39],
- 140 • **Complexity**: are the details of the pressure wave shape felt under the fingers within each heart
 141 beat [40,41]. This behavior can be related to local vasoconstriction and/or dilation of the vessels
 142 as well as the arterial branching system which influences the location of the dicrotic notch as well
 143 as the amplitude of the dicrotic wave. It can be described using spectral entropies and location
 144 and bandwidth of the harmonics of the pulse wave. The shape of the pulse wave can have low,
 145 average or high *complexity* [42,43].

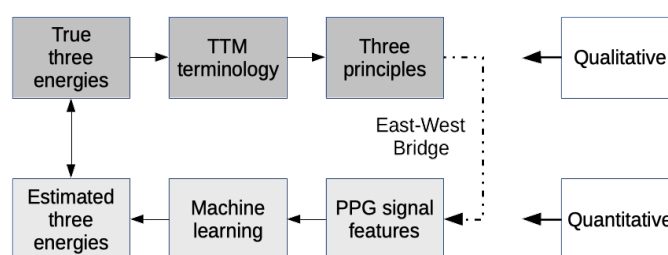
146 Table 2 shows a **qualitative** interpretation of the three energies in function of the three principles
 147 above which are directly connected to the physiological parameters described above. The goal of this
 148 Table is to give the reader an intuitive interpretation of the energies. Each of these principles are further
 149 linked with **quantitative** measures as shown in the Table 3 and described in detail in the Section 4.1.1..

150 The physiological processes involved in the quantification of the three energies can be quite
 151 complex as a nonlinear mix of inter beat intervals variability and pulse wave shape [44]. As a result,
 152 the qualitative interpretation from Table 2 must be turned into a quantitative one using machine
 153 learning techniques as exposed in Section 4.1. The complete flow chart of our work is shown in

Table 2. Relationship between the three energies and principles in terms of physiological parameters

	Stability	Activity	Transformation
Rhythm	Low, Variable	Average, Variable	High, Stable
Force	High	Low	Average
Complexity	Low	High	Average

154 Figure 1 where we clearly distinguish the TTM qualitative path (Traditional Eastern medicine) and the
 155 digital pulse wave analysis path (Technological Western medicine). The true three energies are the one
 156 diagnosed by the Tibetan physician, while the estimated ones are those derived from our algorithm.

**Figure 1.** East-West bridge flow chart

157 3. Methods

158 The paper presents two studies that were conducted in two different countries at different times.
 159 The first study was conducted in Italy between 2008 and 2010. The purpose of the study was to
 160 investigate the use of PPG signals as a tool for analyzing the pulse wave in a similar way as a Tibetan
 161 doctor does. The final aim was to develop a PPG-based classification of the three energies. The second
 162 study was elaborated and realized at St Thomas Hospital in London in 2018 and was designed for the
 163 analysis of the pulse wave during periods of mental stress and relaxation. This second study served as
 164 a validation of the first study and additional analysis of the pulse wave harmonics.

165 Both studies conform with the seventh declaration of Helsinki (2013) on ethical principles
 166 regarding human experimentation developed for the medical community by the World Medical
 167 Association (WMA).

168 3.1. Study 1: Digital Tibetan Pulse Reading

169 3.1.1. Subjects

170 The subject pool consisted in 34 healthy participants (between 18 and 65 years of age, Male (13),
 171 Female (21)) engaged in studies at the Lama Tzong Khapa (Pomaia, Italy). Each participant gave an
 172 informed consent to this study and received an identification code (ID) to preserve privacy, and data
 173 from each subject was kept anonymously. This ID is used to identify the doctor assessment sheets,
 174 pulse wave recordings and clinical measurements. Amongst the 34 subjects, we have the following
 175 fairly equally distributed typology: Activity (14), Transformation (8) and Stability (12). The inclusion
 176 criteria were as follows: Healthy subjects, having a relation with the Institute Lama Tzong Khapa
 177 and/or living in the residential area close by, and willing to be enrolled for the entire duration of this
 178 study. Physical and mental health was ascertained by the medical doctor and psychologist in charge of
 179 this project. Exclusion criteria were as follows: Hypertension level 2 (Systolic >160 mmHg and/or

180 Diastolic $> 95 \text{ mmHg}$ without medication), Cardiovascular problems, Cancer, Diabetes, Breathing
 181 disorders, Mental illness such as schizophrenia, phobias, etc. Participants were given clinical advice
 182 after the study period, so that they are compensated for having participated in the study.

183 3.1.2. Protocol

184 At the time of the enrolment, participants were asked to complete a questionnaire with their
 185 background relevant data, such as age, gender, height and weight. Data were anonymised. According
 186 to Tibetan Medicine, the typology assessment requires the medical doctor and the patient to respect
 187 certain rules such as: diet and behavior the day before the reading and the time of the day which
 188 is traditionally early morning or at dawn when the outer and inner elements are the most balanced.
 189 Due to logistical constrains and the number of participants, we had to adapt these traditional rules by
 190 relaxing the time of day. The Tibetan doctor can slightly adjust his pulse diagnosis according to the
 191 time of when the assessment is done. The participants were asked to behave calmly and avoid eating
 192 spicy food and excitants the day prior to the recording. Routine subject information were recorded
 193 and done continuously during the study. When the participants visited the Tibetan doctor, they had
 194 a Tibetan pulse reading, which was immediately followed by our pulse wave sensor recording as
 195 described in Section 3.1.3. The total recording session were 30 minutes: 15 minutes for the Tibetan
 196 finger pulse reading and 3 to 5 minutes for the pulse wave recording. We used such a short recording
 197 time in order to avoid muscle tension, movement and sweating artefacts as much as possible.

- 198 1. Physiological measurements: blood pressure was measured using a standard automatic
 199 commercial oscillometric system (Omron IA2): systolic, diastolic and heart rate were reported
 200 and recorded on the Tibetan Doctor File (see Section 3.1.3),
- 201 2. Self-report: participants were asked to regularly fill a multiple choice report on temporary
 202 non-compliance, exercise, personal meditation practice, diet, work or study load.

203 The Tibetan doctor file was prepared with the help of Dr. Tsewang Tamdin director of the Men
 204 Tsee Khang Institute (Dharamsala, India) and his collaborators, and Dr. Nida Chenagtsang (director of
 205 the International Academy for Traditional Tibetan Medicine). The file contained information about the
 206 pulse reading as well as any information that the doctor felt necessary and useful for this study such
 207 as sleep and environment/social problems. This was important as this study lasted for a long period
 208 of time.

209 3.1.3. Pulse Wave Recording and Preprocessing

210 The Tibetan pulse information can be measured sequentially with one finger at a time as well as
 211 simultaneously with the three fingers as shown in Figure 2 and is traditionally assessed by the fingers'
 212 feeling of the doctor, placed along the radial artery. Each fingertip, index, middle and ring, assess
 213 different parts of the body: upper, middle and lower respectively. The index finger position is called
 214 *Tson* and corresponds to the Activity energy, the middle finger is called *Kan* and corresponds to the
 215 Transformation energy, and the ring finger is called *Chag* and corresponds to the Stability energy. The
 216 index is always placed toward the thumb in a flat position so that each side of the fingertip can sense
 217 the pulse wave. Left and right wrist pulse reading were taken.

218 Measurements performed by our pulse wave recording system rely on the photoplethysmogram
 219 (PPG). PPG is an optical non-invasive technology allowing the assessment of information related to
 220 subcutaneous blood circulation. By illuminating a living tissue with a light source, PPG can measure
 221 both arterial blood volume changes and blood content [45]. PPG measurements setups consist in
 222 a light source, a photo-diode and the electronics for signal conditioning and filtering. Our optical
 223 probe included a Light Emitting Diode (LED) emitting at 940 nm , and a photodiode located 1 cm
 224 apart. The electronic box includes an analog front-end (performing the continuous removal of ambient
 225 light reaching the photo-diode, and acquiring the raw optical signals 50 times per second (sampling
 226 frequency $F_s = 50\text{Hz}$) via a 24 bits Analog to Digital Converter). Raw optical signals were transmitted

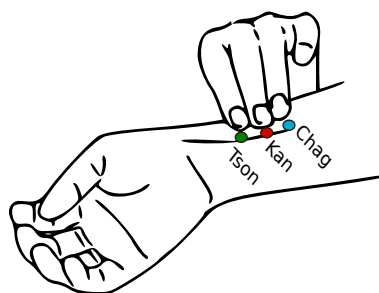


Figure 2. TTP doctor fingers position.

227 via an USB cable to a laptop where data were displayed and stored for further processing. The PPG
 228 signal was further upsampled to 100 Hz for further analysis. Left and right wrist PPG signals were
 229 recorded sequentially.

230 The sensor was made for single finger position measurement at a time and we used the index
 231 finger position. The index finger location is the one proximal to the thumb as can be seen in Figure 2.
 232 This location is particularly suited to analyze the properties related to the heart, lungs, small and large
 233 intestines. The sensor was then positioned on the radial artery in a similar way a Tibetan doctor would
 234 sense the pulse until the signal showed some stability as displayed on the screen of the computer
 235 running the recording software. Once an optimal position was found, the sensor was maintained
 236 with a wrist band during the duration of the recording. The PPG signals were analyzed off-line using
 237 Matlab software (MathWorks, Inc., Natick, Massachusetts, United States).

238 The PPG signal contained a large DC offset, slow drift and movement artefacts despite the
 239 instruction to the subject not to move the hand. Additionally, infrared sensor signals are known to
 240 be more susceptible to deep tissue structure which act as noise sources. The preprocessing consists
 241 in reducing these effects while keeping the main features of the pulse wave [46–48]. We used a
 242 quadratic detrending followed by Principal Component Analysis in State Space (PCA-SS) [49,50] with
 243 an additional frequency selection. The quadratic detrending was performed by removing a piecewise
 244 2nd order polynomial fit to the data by block length of 10s. The PCA-SS was performed using a state
 245 space embedding of the time series with an embedding dimension of $m = 40$ and reconstruction lag
 246 $l = 1$ sample [?]. We selected the first 8 components corresponding to the largest eigenvalues of the
 247 trajectory matrix, thus reducing the amplitude of the high frequencies. We further selected from these
 248 components those for which the spectral content had a maximum between 0.05Hz and 12Hz. This
 249 choice of the frequency band corresponds to the physiologically plausible content of the pulse wave
 250 main harmonics. We have further used a wavelet based noise reduction method [48,51] which finally
 251 resulted in the preprocessed pulse wave signal $DPW(t)$.

252 3.2. Study 2: Mental Stress

253 The mental stress protocol has been presented in details in [11] and is briefly reproduced here for
 254 sake of ease of reading of this article.

255 3.2.1. Subjects

256 Ten young, healthy participants (4 males and 6 females, age range 23 – 31 years, BMI range 17.6 –
 257 33.8 $kg\ m^{-2}$) participated in the study at St Thomas' Hospital, London. All participants completed a
 258 preliminary questionnaire about cardiovascular and mental health as well as any medications that
 259 could influence the results. Exclusion criteria were: diagnosed hypertension, heart arrhythmias,
 260 cognitive impairments. The NRES Committee London – Westminster approved the study IRAS ID

261 (168545) and REC reference (15/LO/1173). Participants could ask to withdraw or pause at any time
 262 during the study. Subjects received an ID code to preserve anonymity.

263 3.2.2. Protocol

264 The study protocol consisted of six phases as illustrated in Figure 3: instrumentation, baseline
 265 measurements, Stroop test 1, relaxation phase, Stroop test 2, and recovery. Blood pressure (BP)
 266 measurements and subjective stress assessment using a visual analog scale (VAS) were performed
 267 before and after each protocol phase. The study was conducted in a dedicated room, isolated from
 268 noise and other visual disturbances. The study phases are described next.

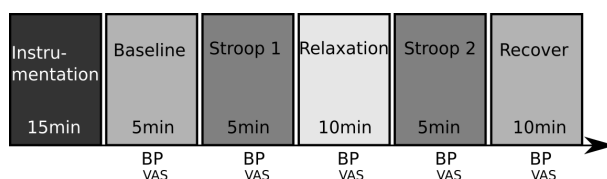


Figure 3. The six phases of the stress study. BP: Cuff blood pressure measurement; VAS: Visual analog scale for subjective stress assessment

269 During the *Instrumentation phase*, participants were provided with instructions on how to perform
 270 the Stroop test and relaxation phases, and measurement instruments were attached (as explained in
 271 the next section). As part of the routine clinical protocol at the hospital, participants completed the
 272 Patient Health Questionnaire (PHQ-9) [52]. The *Baseline phase*, consisted of acquiring measurements
 273 from participants whilst lying on a bed, head tilted up slightly, for five minutes whilst breathing
 274 spontaneously. In the *Stroop test 1 phase*, stress was induced using the color word Stroop test [53]. This
 275 test has been shown to provide reasonable results in terms of controlled induced stress and is widely
 276 used in psychology research. The test was performed for five minutes while subjects were lying down
 277 in the bed looking at a computer screen where the Stroop test was running. Participants were asked to
 278 answer simple word-color-matching questions, at an increasingly faster pace as the test progressed
 279 to compensate for the known adaptation process that participants undergo. In the *Relaxation phase*,
 280 participants used the Resperate system (Resperate, Inc) for ten minutes, which is designed to lower
 281 blood pressure through device-guided slow-paced breathing [54]. The breathing frequency range was
 282 adjusted for each individual according to his comfort zone. In the *Stroop test 2 phase*, a second Stroop
 283 test was conducted lasting five minutes. In the *Recovery phase*, participants relaxed, unaided and in
 284 silence, for ten minutes whilst isolated by a curtain. Reference assessments of stress were obtained at
 285 the end of each phase by asking participants two questions: (i) do you feel any pain or discomfort?;
 286 and (ii) how would you rate your stress level? Subjects provided responses using a VAS ranging from 0
 287 to 10. The VAS has been successfully used in many psychological studies and has the great advantage
 288 of being very simple, especially during experiments when subjects are psychologically stressed [55].

289 3.2.3. Pulse Wave Recording and Preprocessing

290 PPG signals for pulse wave analysis were acquired using OH1 sensors (Polar Electro Oy) placed
 291 on the lateral site of the of the left upper arm. The OH1 device complies with electro-magnetic radiation
 292 safety, has been tested for skin biocompatibility. The OH1 sensor consists of a hexagonal arrangement
 293 of green light sources and measures PPG signals at 135 Hz. The digitalized PPG signal was further
 294 band passed filtered with a linear 4th order Butterworth filter with cutoff frequencies 0.2Hz - 15Hz.
 295 The quality of the PPG signal was far superior to the one used in the first study and thus required less
 296 preprocessing. The preprocessed PPG is called $DPW(t)$.

297 4. Results

298 4.1. Study 1: Digital Pulse Wave Classification

299 4.1.1. Feature Extraction

300 The PPG signal processing flow is summarised in Figure 4. It contained information about the
 301 **Rhythm, Force** and **Complexity** as described in Table 3. The features were computed from both
 302 the heart inter-beat intervals and the preprocessed PPG signal. All features were extracted using a
 303 rectangular sliding window of 30s with 50% overlap.

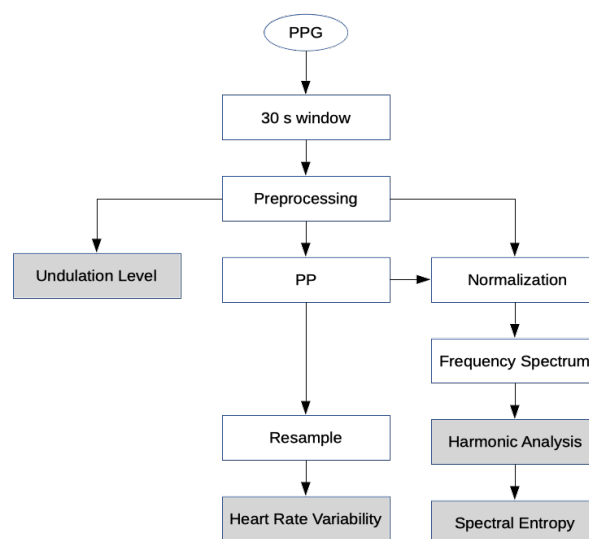


Figure 4. Pulse wave algorithm

304 **Heart rate and linear heart rate variability:** The PPG signal displayed fluctuations both in the
 305 frequency and amplitude domains. The fluctuations in the frequency domain are linked with known
 306 phenomena originating from the neuro-cardiovascular system such as respiration or emotions [56].

307 A peak detection algorithm was used to detect each diastolic point $P(k)$ from $DPW(t)$ at the
 308 heart beat k , and then derive the peak to peak intervals $PP(k) = P(k) - P(k - 1)$. The peak detection
 309 algorithm consists in three steps: a Butterworth 4th order band-pass filter with cutoff frequencies 0.3Hz
 310 and 3Hz is applied to $DPW(t)$ followed by a first order derivative filter and an adaptive peak detection
 311 method. The Butterworth filter removes most of the high and low frequency noise. The slope of the
 312 $DPW(t)$ during the systole phase is characteristically high which results in a sharp peaked signal after
 313 the derivative. The adaptive peak detection method described in [57] was used to finally find the peaks.
 314 Spline interpolation around the detected peaks was further used to increase the peaks location accuracy.
 315 Please note that the location of the derivative peaks are not the location of the $DPW(t)$ systolic foot
 316 which can be easily located by looking backward to the next local minima. We have used a technique
 317 to automatically detect and eventually correct non-physiological PP intervals or ectopic beats [58]. The
 318 fluctuations of these PP intervals have been shown to be similar to the electrocardiogram peak R-wave
 319 intervals variability [59] for healthy subjects at rest and are thus suitable for our analysis. The interbeat
 320 intervals PP were quantified using their average value and variability: 1) the average pulse PPm , 2) the
 321 variance Rv , 3) the normalised Low Frequency (LF) Power (LFn : power in 0.04 Hz to 0.15 Hz) and 4)
 322 the normalised High Frequency (HF) Power (HFn : power in 0.15 Hz to 0.4 Hz). The normalisation of
 323 the LF and HF was performed by dividing them by the total power of the DC free PPG segment under
 324 analysis. Breathing is an important modulation factor both in the PPG amplitude and frequency, i.e.

325 the so-called Respiratory Sinus Arrhythmia (RSA). The RSA is usually measured from the PP interval
 326 in the frequency band from 0.1 Hz to 0.25 Hz when the person is in a calm spontaneous breathing state
 327 as typically the case when visiting a doctor. The breathing frequency BF was thus estimated as the
 328 frequency corresponding to the maximum frequency spectrum peak in this band.

329 **Harmonic analysis:** The pulse wave contains a rich spectrum which is essentially related to the
 330 different functions of the heart, vascular, autonomic nervous and respiratory systems, as well as
 331 other components from the different organs visited by this wave. In order to isolate the vascular part
 332 contained in the shape of each heart beat without the 'interference' of the heart beat variability, we have
 333 implemented a technique to normalise each heart beat pulse wave so that they have the same peak
 334 peak amplitude of 1 and same duration of 1s [38]. From the knowledge of the peak wave instant $P(k)$,
 335 the procedure was performed in three steps: 1) to detrend each heart beat so that each diastolic points
 336 have zero amplitude, 2) to resample each heart beat wave using a linear interpolation method, and 3)
 337 to normalise each heart beat to an amplitude of 1. Once this procedure is performed on each heart
 338 beat pulse wave, we performed a spectral analysis and derive the power spectral density $P(\omega)$. We
 339 have used a Welch method to estimate the power spectrum density. The number of harmonics Nb^H
 340 contained in $P(\omega)$, their amplitudes A_k^H , locations f_k^H , phases ϕ_k^H and bandwidths Δ_k^H , $k = 1, \dots, Nb^H$,
 341 were the main used spectral features. The fundamental frequency f_0^H corresponds to the heart beat
 342 average frequency: i.e. the heart rate. The bandwidth Δ_k^H of a signal x , centred around the frequency
 343 f_k^H , was computed as follows:

$$\Delta_k^H = \sqrt{\int_{\Omega} \tilde{P}(\omega) (\omega - 2\pi f_k^H)^2 d\omega} \quad (1)$$

344 where Ω is the bandwidth of interest and $\tilde{P}(\omega)$ is an estimation of the energy-normalised power
 345 spectral density of $DPW(t)$: $\tilde{P}(\omega) = P(\omega) / \int_{\Omega} P(\omega) d\omega$. The bandwidth of the fundamental frequency
 346 is $BW = \Delta_0^H$. The parameter BW is thus proportional to the variance of the PP intervals, while $\Delta_{k>0}^H$
 347 measure the variability of the smaller waves composing the heart pulse wave $DPW(t)$. The frequencies
 348 $f_{k>0}^H$ and phases $\phi_{k>0}^H$ are modulated by the arterio-venous tree properties such as branching (anatomy)
 349 and wall (i.e. endothelium) structures. These aspects are known to influence the shape of the pulse
 350 wave such as the crest time, dicrotic notch location and amplitude and dicrotic wave amplitude. Thus
 351 the frequency domain analysis is an other way to measure the influence of the anatomical, functional
 352 and local nervous system properties of the vessels. Mathematically, the Fourier transform of a signal
 353 contains exactly the same information as the time domain which further justify the use of the frequency
 354 analysis of the pulse wave. This harmonic frequency analysis has been studied by Chinese medical
 355 doctors [43,60,61] and scientists since years and are known to correlate with organ function as well. The
 356 amplitude of the PPG signal is usually not calibrated thus limiting the use of the absolute amplitude or
 357 power of such signal. However, the relative power using ratios of harmonics is relevant and indeed
 358 contains known health information [43,61–63]. In our work we will limit the number of harmonics to
 359 $Nb^H = 4$ and we use the harmonic power ratios as features: $H_{i,j} = A_i^H / A_j^H$ for $i, j = 0, \dots, Nb^H$ with
 360 $j > i$. One of the main advantage of using the harmonic analysis is that it is more easy and robust to
 361 compute than time domain parameters in the presence of noise.

362 **Order analysis:** A well known measure of regularity or order is entropy. The regularity of the pulse
 363 wave shape is relevant for our study and can be quantified using spectral entropy. Typically, narrow
 364 frequency band signals will have a small entropy as compared to broadband signals. The normalised
 365 Spectral Entropy (SE) in Ω is defined as:

$$SE = - \left(\int_{\Omega} \tilde{P}(\omega) \log(\tilde{P}(\omega)) d\omega \right) / \Omega \quad (2)$$

Table 3. Digital Pulse Wave Qualities and Features

DPW Qualities	DPW Features
Rhythm	Normalized PP Low Frequency (LFn)
	Normalized PP High Frequency (HFn)
	PP Variance (Rv)
	PP Average (Rm)
	Breathing Frequency (BF)
Force	Undulation Level (UL)
Complexity	Normalized Bandwidth (BW)
	Normalised Spectral Entropy (SE)
	Harmonic Ratios ($H_{i,j}$)

366 The regularity of the pulse wave in the time domain is characterised in first approximation by an
367 Undulation Level (UL). The pulse wave is indeed modulated in amplitude due to various factors such
368 as respiration, the autonomous nervous system or heart pacemaker dysrhythmias. The UL is also well
369 adapted to measure the depth of modulation during RSA, and thus the influences of the respiration on
370 the pulse wave amplitude fluctuations. The concept of the modulation depth used in this context is
371 borrowed from the domain of telecommunication where the modulation depth is defined from the
372 following equation:

$$x(t) = K(1 + UL \cos(\omega_{AM}t)) \cos(\omega_{FM}t) + n(t) \quad (3)$$

373 where $\omega_{AM,FM}$ is the angular frequency of the (Amplitude,Frequency) modulated part of $x(t)$ and $n(t)$
374 is some zero mean noise. The modulation depth UL varies between 0 and 1. The estimation of UL can
375 be performed using demodulation methods.

376 4.1.2. Features Selection and classification

377 **Features Selection:** In Table 3, the $9 + Nb^H(Nb^H)/2$ features are summarized. In order to condition our
378 feature space in the best way, we have proceeded to a feature selection procedure. A method developed
379 by Peng *et al.* [64] called mRMR (minimum Redundancy Maximum Relevance Feature Selection) has
380 been chosen and applied to our feature set. The mRMR method need the feature values to be converted
381 to symbols. In order to do this, we have quantized the features using a standard quantization method
382 on 5 bits. Each quantized level is then assigned an integer value, which together with the classes are
383 the input to mRMR. The result of mRMR is summarized as follows where the features have to be read

384 from left to right and are in order of decreasing minimum redundancy. Progressively grouped features
385 from left to right also have decreasing minimum redundancy.

$$\mathbf{Rv} \rightarrow \mathbf{SE} \rightarrow \mathbf{H}_{2,4} \rightarrow \mathbf{H}_{1,2} \rightarrow \mathbf{UL} \rightarrow \mathbf{Rm}$$

386 Due to the limited number of subjects and $DPW(t)$ signal duration, the number of feature points
387 is quite limited. In order to improve the robustness of the classification, we have decided to make
388 use of surrogates of the features. The way to produce high quality surrogates is explained in detail
389 in [65]. Using Schreiber method as a first step, we have improved the surrogate by making them
390 probability density function invariant as well. This second step guarantees that the surrogates' pdfs are
391 preserved. This surrogate method is further used in this work to test the performance of the classifier
392 by using Monte Carlo simulations of the classifier (see Section 4.1.2). In order to further ease the work
393 of the classifier, we have performed a Principal Component Analysis in State Space (PCA-SS). The
394 parameters for the nonlinear embedding are: dimension $m = 4$ and lag $l = 1$. The first 4 Principal
395 Components have been retained.

396 **Classification of the Three Energies:** As explained in Section 2.1 each individual possesses a dominant
397 Typology and sometimes manifest the other two in different proportions. The classification of the
398 typology must thereby take this into account, which impose a classifier with continuous output
399 values rather than binary. Fuzzy classifiers thus seems the most appropriate. Amongst the fuzzy
400 classifiers, a special type of Artificial Neural Networks called Quantum Neural Networks (QNN)
401 have shown promising properties [66]. These QNNs are a class of feedforward neural networks
402 which can handle uncertain inputs and have a very flexible structure of hidden nonlinear layer in
403 the form of a superimposition of sigmoidal functions with flexible amplitude, slope and shift. The
404 hidden layer can focus or relax its *data representation* by concentrating or spreading around regions
405 of certainties or uncertainties of the feature space more like a quantum wave function localize or
406 spread out around certain or uncertain states bearing some resemblance to quantum systems and
407 networks. Forty surrogate PCA-SS components are generated to train the QNN with one hundred
408 batch iteration. We have validated the trained network using additional independent surrogated data.
409 These validation surrogates are then used to compute the Receiver Operating Curves (ROC) of the
410 QNN in a Monte Carlo simulation and an optimal threshold is found using the Youden index [67]. The
411 confusion matrix is then computed from these Monte Carlo simulations at the Youden optimal point.
412 The confusion matrix C expressed in percent is given as:

$$C = \begin{pmatrix} C_{1;1} & C_{1;2} \\ C_{2;1} & C_{2;2} \end{pmatrix} \quad (4)$$

413 The diagonal entries $C_{1(2);1(2)}$ are related to the percent of samples which are correctly classified
414 in the respective Class 1(2). The off-diagonal entries in C have the following meaning: $C_{1(2);2(1)}$ is
415 the percentage of samples from Class 1(2) which are classified as Class 2(1). The confusion matrix
416 (4) has the following standard statistical meaning: for Class 1(2), $C_{1(2);1(2)}$ are the True Positive Rates
417 (respectively True Negative Rates), and $C_{1(2);2(1)}$ are the False Negative Rates (respectively False
418 Positive Rates) such that $C_{1(2);1(2)} + C_{1(2);2(1)} = 100$. The Sensitivities and Specificities for Class 1(2) are
419 thus $Sen_{1(2)} = C_{1(2);1(2)}$ and $Spec_{1(2)} = C_{2(1);2(1)}$ respectively. Please note that in our 2-class problem,
420 Sensitivity and Specificity are symmetrical. When assessing the performance of the classifier, we aim
421 at maximizing the diagonal elements, while minimizing the off diagonal elements, ideally 100% and
422 0% respectively.

423 The classification is performed in two steps using two classifiers: Step 1: Separation of *Activity*
424 from *Transformation* and *Stability* and Step 2: Separation of *Transformation* from *Stability*. This has
425 proved to be the best strategy to maximize the classifier performances. The first classifier is called
426 QNN First Pass (FP): QNN^{FP} . By assumption we assign Class 1 to *Activity*, while Class 2 is the union

427 of Transformation and Stability: (Transformation - Stability). The confusion matrix at the optimal ROC
 428 point C^{FP} of the QNN^{FP} is given as:

$$C^{FP} = \begin{pmatrix} C_{1,1}^{FP} = 85(2) & C_{1,2}^{FP} = 15(2) \\ C_{2,1}^{FP} = 28(2) & C_{2,2}^{FP} = 72(2) \end{pmatrix} \quad (5)$$

429 The second classifier is called QNN Second Pass (SP): QNN^{SP} . By assumption we assign Class 1
 430 to Transformation, while Class 2 is Stability. The confusion matrix at the optimal ROC point C^{SP} of the
 431 QNN^{SP} is given as:

$$C^{SP} = \begin{pmatrix} C_{1,1}^{SP} = 90(2) & C_{1,2}^{SP} = 10(2) \\ C_{2,1}^{SP} = 14(2) & C_{2,2}^{SP} = 86(2) \end{pmatrix} \quad (6)$$

432 Our classification results are summarized in Table 5

Table 5. Average Sensitivity and Specificity

	Stability	Activity	Transformation
Sensitivity	86%	85%	90%
Specificity	90%	72%	86%

433 4.2. Study 2: Mental Stress

434 Distributions of parameters across subjects were summarized using the median and inter-quartile
 435 range in box plots. Significant differences between parameters were identified using paired t -Tests
 436 (significance level $\alpha = 0.05$).

437 4.2.1. The Three Energies

438 Figure 5 shows the three energies computed according to the methodology presented above in
 439 each phase of the protocol for the 10 participants. Please note that the humours/energies have no units
 440 as they are the likelihood of each class and are bounded between 0 and 1. Activity and Transformation
 441 increased significantly from baseline to Stroop 1, while Stability stayed almost unchanged. During
 442 the breathing relaxation period, Stability increased significantly with an associated large dispersion
 443 across subjects, while the Activity and Transformation decreased significantly back to baseline. Stroop
 444 2 manifested in a slight nonsignificant increase of Activity and Transformation with respect to baseline,
 445 while Stability decreased significantly from relaxation showing a reduced capacity to cope with stress.
 446 During the recovery period, Activity, Transformation and Stability came back to baseline with a
 447 noteworthy low dispersion of Stability.

448 The statistical analysis is summarized in Table 6 where the significance value $p_{m,n}$ is displayed
 449 with the following index convention: $n, m = 1$ for Baseline, $n, m = 2$ for Stroop 1, $n, m = 3$ for
 450 Relaxation, $n, m = 4$ for Stroop 2 and $n, m = 5$ for Recovery.

Table 6. Statistics for the three energies

Transformation	$p_{1,2} = 1.16 \cdot 10^{-6}; p_{2,3} = 5.43 \cdot 10^{-4}; p_{2,4} = 5.79 \cdot 10^{-4}; p_{2,5} = 2.57 \cdot 10^{-5}$
Activity	$p_{1,2} = 9.45 \cdot 10^{-5}; p_{2,3} = 1.14 \cdot 10^{-3}; p_{2,4} = 2.77 \cdot 10^{-3}; p_{2,5} = 1.62 \cdot 10^{-4}$
Stability	$p_{1,3} = 2.36 \cdot 10^{-2}; p_{3,4} = 1.33 \cdot 10^{-2}; p_{3,5} = 2.50 \cdot 10^{-2}$

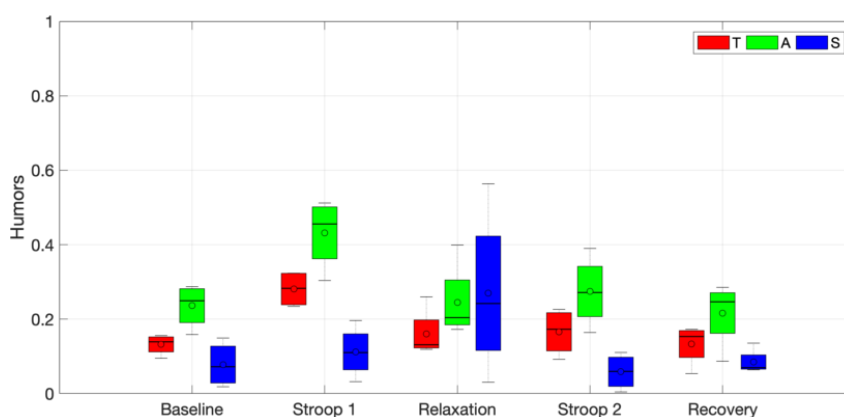


Figure 5. The three energies during the mental stress protocol

4.2.2. Harmonics

It has been suggested in [11] that the complexity of the pulse wave contour could be a further parameter able to discriminate the states of stress. In this continuation, the complexity of a wave can be quantified by its Fourier spectrum, and thus its harmonic content if this wave is periodic or quasi-periodic. As it was introduced in Section 4.1.1, the harmonic analysis proved to be a very efficient way to extract pulse wave structure parameters [43,61,68]. In order to further assess this hypothesis, we have analyzed the behavior of the harmonic ratios $H_{i,j}$ as defined in Section 4.1.1. Figure 6 shows the behavior of $H_{i,j}$ across the stress protocol. The harmonic ratios $H_{i,j}$ are unit-less. From Figure 6, we can observe that the harmonic ratios are changing during the various phases of the protocol, confirming that they contain information according to the stress/relaxation level as manifested by the vascular system. The second striking observation is a clear separation between the low and high harmonic ratios as indicated in Figure 6 by the red and green colored bars respectively. This indicates that the higher the harmonic frequencies the less differences between their amplitude. Visual inspection indicates that the relaxation procedure affects mostly $H_{1,2}$ and $H_{2,4}$ and that mental stress affects $H_{2,4}$ primarily. The highest harmonic ratio $H_{3,4}$ tends to decrease during the protocol.

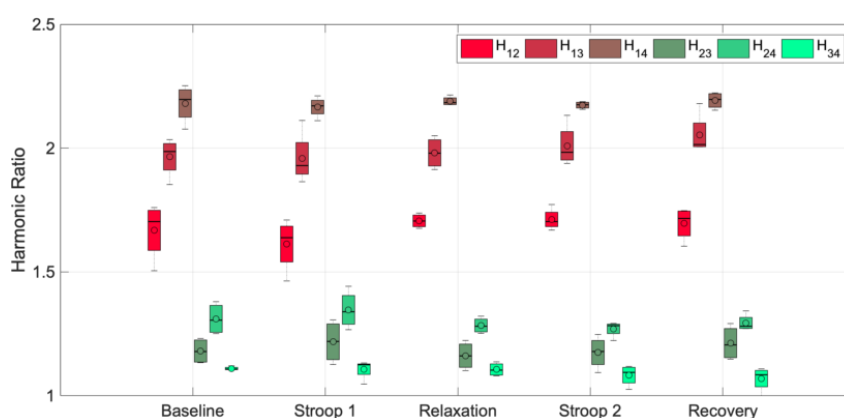


Figure 6. The harmonic ratios during the mental stress protocol

The statistical analysis is summarized in Table 7 with the same convention as above. $H_{2,4}$ and $H_{2,4}$ are thus good candidates for monitoring stress and relaxation. It was also selected by our feature selection algorithm in Section 4.1.1.

Table 7. Statistics for the harmonic ratios

$H_{1,2}$	$p_{2,3} = 2.08 \cdot 10^{-3}; p_{2,4} = 1.92 \cdot 10^{-2}$
$H_{1,3}$	$p_{1,5} = 3.45 \cdot 10^{-2}$
$H_{2,4}$	$p_{2,3} = 3.38 \cdot 10^{-2}; p_{2,4} = 1.29 \cdot 10^{-2}$
$H_{3,4}$	$p_{1,5} = 2.52 \cdot 10^{-2}$

469 We have further tested our hypothesis of the relationship between the time domain pulse wave
 470 analysis as presented in [10,11,69] and the harmonic ratios presented here. For this purpose, we have
 471 produced a simulated PPG based on a linear superposition of two bandpass filtered (Butterworth filter
 472 2nd order with cutoff frequencies 0.3Hz and 4Hz) asymmetric sawtooth signals (shape is shown in
 473 Figure 6(a)). The asymmetrical sawtooth shape controls the systolic and diastolic heart contraction
 474 and relaxation phases, and noteworthy the crest time: i.e. the time from the foot to the peak systole.
 475 We have simulated different PPG with increasing crest time (CT), i.e. the the time delay between the
 476 onset of a pulse wave and the peak of the wave also called tidal wave peak, in the range of our clinical
 477 measurements [11] and performed a Fourier analysis to compute the $H_{1,2}$ and $H_{2,4}$ (continuous curves
 478 in Figure 7(b)). Figure 6(b) shows a very good agreement between the simulation and the clinical
 479 measurement harmonic ratios (color circles in Figure 7(b)).

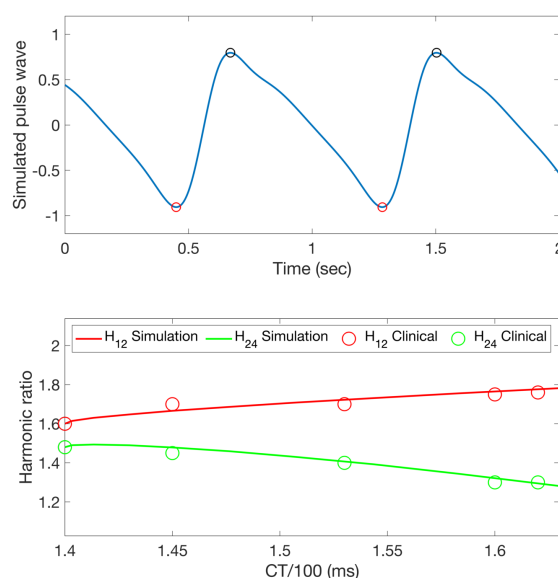


Figure 7. ((a) An example of a synthetic PPG signal with peak systole and diastole. (b) The relationship between the crest time (CT) and the harmonic ratios $H_{1,2}$ and $H_{2,4}$ from Figure 6

480 5. Discussion

481 **The three energies.** We have developed a methodology based on photoplethysmogram (PPG)
 482 pulse wave analysis to estimate the three fundamental energies of Traditional Tibetan Medicine (TTM).
 483 The three fundamental energies or humours described in TTM have been characterized using modern
 484 techniques of PPG analysis, both in time and frequency domains. The TTM pulse reading is essentially
 485 qualitative and holistic like all ancient medicinal systems. This synthetic view of health has been lost in
 486 modern analytical techniques which tend to view health and disease using compartmental approaches.
 487 Despite the success of the diagnostic techniques developed by Western science, there is a resurgence of

488 integrative approaches viewing health in a more holistic way. There is thus a growing demand for
489 using modern techniques of digital processing and machine learning based on ancient knowledge.
490 Practiced by an experienced physician trained in TTM, it is quite challenging to assess the results of
491 the method using quantitative modern techniques. In this work, we have been able to express the TTM
492 pulse reading using the three principles of Rhythm, Force and Complexity. Each of these principles
493 having a direct interpretation in terms of physiological processes as explained in Section 2.2. Moreover,
494 these three principles can be implemented using PPG signals. The signal processing techniques used in
495 this work are not novel by themselves, but their combination gives interesting insights as we combine
496 two different approaches: 1) the beat to beat heart intervals and 2) the pulse wave shape. Both of these
497 aspects are usually analysed separately in the literature for historical and research field application
498 reasons. Similar approaches and aims have been developed from a Chinese pulse reading perspective
499 [21,22] and noteworthy the work of Tang et al. [44] which uses an eight element approach similar to
500 our three principles. The three TTM energies of Stability, Activity and Transformation are derived from
501 the three principles which allowed us to have a holistic view on the human body function: namely the
502 autonomic nervous system, the breathing system and the vascular system. An other approach based
503 on time characteristics of the pulse pressure wave has been applied from an Ayurvedic point of view
504 [17] and was proven useful in relation to arterial stiffness. The use of our approach can specifically be
505 applied to chronic diseases or dysfunctions originating from multiple sources such as stress or sleep
506 disorders, fibromyalgia, multiple sclerosis or mental problems such as ADD/ADHD or chronic stress.

507 **Mental stress and the three energies.** According to TTM, stress is primarily an Activity disorder
508 associated with Transformation imbalance and manifest primarily in the nervous system with high
509 impact on blood pressure and the vascular system. In a previous study, we have shown that time
510 domain pulse wave analysis can be a complimentary tool for the analysis of mental stress specifically
511 the crest time and the diastolic time of the pulse wave [10,11]. Both of these aspects are now mostly
512 encoded in the principle of Complexity whereby a shortened diastolic time and crest time are reflected
513 by an increased Complexity, i.e. increased BW and SE , which according to Table 2 reflect an increased
514 Activity energy. This study further shows that in a state of stress, not only the Activity is increased but
515 the Transformation energy which correspond to an increase of metabolic heat, heart rate and decreased
516 heart rate variability as shown in Table 2. Ayurveda expert Lad [30] also relates the Activity energy
517 (Vata in Ayurveda) to increased artery stiffness. The counter aspect of a stress state is a relax state.
518 Relaxation is dominantly manifested as an increase in Stability energy and decrease in both Activity
519 and Transformation. This is also mentioned by Lad whereby soft arteries related to Kapha: i.e. Stability.
520 Increased levels of Activity and Transformation correspond to increased pulse wave velocity, while
521 normal to low level of Stability energy corresponds to reduced pulse wave velocity. Both pulse wave
522 velocity and arterial stiffness have been shown to correlate with high blood pressure [69? ?]. Figure
523 5 illustrate this point clearly. On a physiological level, this corresponds to a decreased heart rate,
524 increased heart rate variability, decreased arterial stiffness and blood pressure (especially systolic)
525 and increased diastolic time as well as pulse transit time (timing between the main pulse peak and
526 the dicrotic peak) [10,11]. This is again illustrated in our Table 2. The interesting finding is also the
527 adaptation process to stress as shown in the Stress 2 and the recovery phase where the Activity and
528 Transformation energies do not increase as significantly as in Stroop 1, and remain close or slightly
529 decrease to that Stroop 2 state in the recovery phase. This indicates that a laboratory stress test is only
530 a short term exploration of the stress phenomena. Further longer term recording of stressed people is
531 needed to validate any stress quantitative metrics.

532 **Mental stress and the harmonic ratios.** Harmonic ratios have been studied in [43,61] in
533 relationship with the Chinese medicine framework and the organs' function. It would be premature to
534 draw conclusions from our study in relation to the energy/humor theory, but we can however mention
535 that the harmonic ratios $H_{1,2}$ and $H_{2,4}$ could indeed be linked to the relationship between the heart
536 and the lungs, and between the lungs and smaller organs involved in digestion respectively [43]. The

537 harmonic ratios $H_{2,4}$ and $H_{1,2}$ were selected as a salient features for our classifier, thus also showing
538 their relevance in the determination of the energies.

539 Our study further showed that the behaviour of $H_{1,2}$ and $H_{2,4}$ are related to the crest time from
540 our previous analytical and clinical studies [10,11], thus making a bridge between time and frequency
541 domain analysis of the pulse wave. As the crest time is also a good indicator of arterial stiffness [70–72],
542 we can infer that the harmonic analysis can also gives insights into the health of the vascular system.
543 The harmonic analysis can be a very useful tool to assess mental stress as it does not requires the task
544 of detecting the various pulse wave features which can prove to be difficult in some situations [72]
545 such as slight micro-movements, skin condition and perfusion. Additionally, it has been shown that
546 this harmonic analysis is relevant for detecting pathological conditions such as coronary artery disease
547 [63], hypertension [61], myocardial ischemia, decrease of heart function in type II diabetes patients
548 [63].

549 6. Conclusion

550 In this work we have developed an algorithm based on photoplethysmogram for the estimation
551 of the three humors known to be the essential energies governing our body and mind following the
552 Traditional Tibetan Medicine system. In order to facilitate the understanding of these energies, we have
553 tentatively defined Western terms such as Activity, Transformation and Stability. We have developed
554 a strategy to translate the ancient Tibetan terms into three principles that guided us to implement
555 our signal processing analysis. We have further used a classifier to estimate the three energies. The
556 algorithm showed reasonable performances on a small selected set of pulse wave features.

557 We further applied the classifier to the test case of mental stress and active relaxation using paced
558 breathing. Results showed consistent statistics with respect to both Tibetan Medicine interpretation
559 and Western medicine physiological processes. We finally showed interesting results on harmonic
560 analysis of the pulse wave and related our results with the crest time pulse wave feature which is
561 known to be related to arterial stiffness and pulse wave velocity. Eastern medicine is holistic by nature
562 and in our work we have shown the potential use of Traditional Tibetan medicine pulse reading for the
563 assessment of mental stress and breathing relaxation techniques. Our digital sensing and processing
564 approach is not aimed at replacing a qualified traditional physician but rather to give an additional
565 tool for his assessment.

566 Several stress management interventions have been shown to be effective in both the workplace
567 and personal settings [73]. This provides great incentive for developing wearable sensing and
568 processing techniques to recognise elevated stress levels, prompting interventions to reduce stress
569 levels, and potentially improve health. Eventually, our approach can be useful to this purpose, and
570 also to complex chronic multi-source illnesses as well as a preventative tool for monitoring the quality
571 of life.

572 Both traditional and modern medical systems have advantages and drawbacks, and certainly
573 can benefit from each other. Specifically, traditional medicine would benefit from the technological
574 advances of modern diagnostic tools.

575 7. Patents

576 A patent named: A method and system for determining the state of a person on the classification
577 of the three humours, has been filed under EP2874539 and WO 2014/012839.

578 **Author Contributions:** Conceptualization, Patrick Celka; methodology, Patrick Celka and Marina Brucet;
579 software, Patrick Celka; Tibetan pulse diagnosis, Lobsang Samten; formal analysis, Patrick Celka; clinical analysis,
580 Abdullah Alabdulgader; environmental impact analysis, Abdullah Alabdulgader; investigation, Marina Brucet
581 and Patrick Celka; writing–original draft preparation, Patrick Celka, Abdullah Alabdulgader; writing–review and
582 editing, Patrick Celka, Abdullah Alabdulgader; supervision, Marina Brucet; project administration, Marina Brucet

583 **Funding:** The mental stress study was supported by a project grant from the British Heart Foundation
584 (PG/15/104/31913) and the Wellcome/EPSRC Centre for Medical Engineering at King's College London (WT

203148/Z/16/Z). Polar Electro Oy partly financed this study. The views expressed are those of the authors and not necessarily those of the Wellcome Trust or EPSRC.

Acknowledgments: We would like to thanks Dr Nida Chenagtsang (International Academy for Traditional Tibetan Medicine) for his constant support during this project. Many thanks to the Swiss Center for Electronics and Microtechnology (csem SA, Neuchâtel) to have prepared the photoplethysmograph sensor along with the software allowing to digitise the data. We also would like to thanks King's College for allowing us to access the OH1 stress study data. Many thanks to Rollin McCraty for the many discussions we had about this work.

Conflicts of Interest: P. Celka was an employee of Polar Electro Oy at the time of the mental stress study and declare no conflict of interests. Other authors declare no conflict of interests.

594

- 595 1. Brotman, D.J.; Golden, S.H.; Wittstein, I.S. The cardiovascular toll of stress, 2007.
- 596 2. Bolger, N.; DeLongis, a.; Kessler, R.C.; Schilling, E.a. Effects of daily stress on negative mood. *Journal of personality and social psychology* **1989**.
- 597 3. Khansari, D.N.; Murgu, A.J.; Faith, R.E. Effects of stress on the immune system, 1990.
- 598 4. McGrady, A. Psychophysiological mechanisms of stress. *Principles and practice of stress management* **2007**,
- 599 3, 16–37.
- 600 5. Allen, J. Photoplethysmography and its application in clinical physiological measurement. *Physiological measurement* **2007**, 28, R1.
- 601 6. Tuchin, V. *Handbook of Optical Biomedical Diagnosis*; SPIE Press, 2002.
- 602 7. Cavalcante, J.L.; Jac, L.; Redheuil, A.A.M. Aortic stiffness current understanding and future directions. *J Am Coll Cardiol* **2011**, 57, 1511–1522.
- 603 8. Heffernan, K.S.; Karas, R.H.; Patvardhan, E.A.; Jafri, H.; JT, K. Peripheral arterial tonometry for risk stratification in men with coronary artery disease. *Clin Cardiol* **2010**, 33, 94–98.
- 604 9. Prince, C.T.; Secrest, A.M.; Mackey, R.H.; Arena, V.C.; Kingsley, L.A.; others. Pulse wave analysis and prevalent cardiovascular disease in type 1 diabetes. *Atherosclerosis* **2010**, 213, 469–474.
- 605 10. Charlton, P.H.; Celka, P.; Farukh, B.; Chowienczyk, P.; Alastruey, J. Assessing mental stress from the photoplethysmogram: A numerical study. *Physiological Measurement* **2018**, 39, 054001.
- 606 11. Celka, P.; Charlton, P.; Farukh, B.; Chowienczyk, P.; Alastruey, J. Influence of mental stress on the pulse wave features of photoplethysmograms *The Institution of Engineering and Technology, Healthcare Technology Letters*, **2019**, under review
- 607 12. Zangróniz, R.; Martínez-Rodrigo, A.; López, M.; Pastor, J.; Fernández-Caballero, A. Estimation of Mental Distress from Photoplethysmography *Applied Sciences*, **2018**, 8 69–84.
- 608 13. Madhan Mohan, P.; Nagarajan, V.; Das, S. R. Stress measurement from wearable photoplethysmographic sensor using heart rate variability data *In International Conference on Communication and Signal Processing, ICCSP 2016*, **2016**, 2016 11141–1144.
- 609 14. Minakuchi, E.; Ohnishi, E.; Ohnishi, J.; Sakamoto, S., Hori, M., Motomura, M.; Hoshino, J.; Murakami, K.; Kawaguchi, T. Evaluation of mental stress by physiological indices derived from finger plethysmography *Journal of Physiological Anthropology*, **2013**, 32 17–28.
- 610 15. Kageyama, Y.; Odagaki, M.; Hosaka, H. Wavelet analysis for quantification of mental stress stage by finger-tip photo-plethysmography *In Annual International Conference of the IEEE Engineering in Medicine and Biology*, **2007**, 2007 1846–1849.
- 611 16. Nelson, M.; Stepanek, J.; Cevette, M.; Covalciuc, M.; Hurst, R.; others. Noninvasive measurement of central vascular pressures with arterial tonometry: Clinical revival of the pulse pressure waveform? *Mayo Clin Proc* **2010**, 85, 460–472.
- 612 17. Nelson, M.; Stepanek, J.; Cevette, M.; Covalciuc, M.; Hurst, R.; others. Significance of arterial stiffness in Tridosha analysis: A pilot study *Journal of Ayurveda and Integrative Medicine* **2017**, 8, 252–256.
- 613 18. Zarshenas, M.M.; Abolhassanzadeh, Z.; Faridi, P.; Mohagheghzadeh, A. Sphygmology of ibn sina, a message for future. *Heart views: the official journal of the Gulf Heart Association* **2013**, 14, 155.
- 614 19. Nasser, M.; Tibi, A.; Savage-Smith, E. Ibn Sina's Canon of Medicine: 11th century rules for assessing the effects of drugs. *Journal of the Royal society of Medicine* **2009**, 102, 78–80.
- 615 20. Chudakova, T. The Pulse in the Machine: Automating Tibetan Diagnostic Palpation in Postsocialist Russia. *Comparative Studies in Society and History* **2015**, 57, 407–434.
- 616
- 617
- 618
- 619
- 620
- 621
- 622
- 623
- 624
- 625
- 626
- 627
- 628
- 629
- 630
- 631
- 632
- 633
- 634
- 635
- 636

- 637 21. Velik, R. An objective review of the technological developments for radial pulse diagnosis in Traditional
638 Chinese Medicine. *European Journal of Integrative Medicine* **2015**, *7*, 321–331.
- 639 22. Luo, C.H.; Chung, Y.F.; Hu, C.S.; Yeh, C.C.; Si, X.C.; Feng, D.H.; Lee, Y.C.; Huang, S.I.; Yeh, S.M.; Liang,
640 C.H. Possibility of quantifying TCM finger-reading sensations: I. Bi-sensing pulse diagnosis instrument.
641 *European Journal of Integrative Medicine* **2012**, *4*, e255–e262.
- 642 23. Kim, H.; Kim, J.Y.; Park, Y.J.; Park, Y.B. Development of pulse diagnostic devices in Korea. *Integrative
643 medicine research* **2013**, *2*, 7–17.
- 644 24. Donden, Y. *Health through balance: An introduction to Tibetan medicine*; Motilal Banarsidass Publ., 2003.
- 645 25. Norbu, N. *On Birth and Life - A Treatise on Tibetan Medicine*; Shang-Shung Edizioni, 1983.
- 646 26. Clark, B. *The Quintessence Tantras of Tibetan Medicine*; Snow Lion Publications, 1995.
- 647 27. Lad, V. *Ayurveda: The science of self-healing: A practical guide*; Lotus press, 1984.
- 648 28. Ni, M. *The Yellow Emperor's Classic of Medicine: A new translation of the Neijing Suwen with commentary*;
649 Shambhala Publications, 1995.
- 650 29. Wang, Y.Y.L.; Wang, S.H.; Jan, M.Y.; Wang, W.K. Past, Present, and Future of the Pulse Examination. *Journal
651 of traditional and complementary medicine* **2012**, *2*, 164–177.
- 652 30. Lad, V. *Secrets of the Pulse: The Ancient Art of Ayurvedic Pulse Diagnosis*; Motilal Banarsidass;; 2nd edition,
653 2007
- 654 31. Nichols, W.W. Clinical measurement of arterial stiffness obtained from noninvasive pressure waveforms.
655 *American journal of hypertension* **2005**, *18*, 3S–10S.
- 656 32. Couceiro, R.; Carvalho, P.; Paiva, R.; Henriques, J.; Quintal, I.; Antunes, M.; Muehlsteff, J.; Eickholt, C.;
657 Brinkmeyer, C.; Kelm, M.; others. Assessment of cardiovascular function from multi-Gaussian fitting of a
658 finger photoplethysmogram. *Physiological measurement* **2015**, *36*, 1801.
- 659 33. Goshvarpour, A.; Goshvarpour, A. Poincaré's section analysis for PPG-based automatic emotion
660 recognition. *Chaos, Solitons & Fractals* **2018**, *114*, 400–407.
- 661 34. Li, F.; Yang, L.; Shi, H.; Liu, C. Differences in photoplethysmography morphological features and feature
662 time series between two opposite emotions: Happiness and sadness. *Artery Research* **2017**, *18*, 7–13.
- 663 35. Choi, A.; Shin, H. Photoplethysmography sampling frequency: pilot assessment of how low can we go to
664 analyze pulse rate variability with reliability? *Physiological measurement* **2017**, *38*, 586.
- 665 36. Shaffer, F.; Ginsberg, J. An overview of heart rate variability metrics and norms. *Frontiers in public health*
666 **2017**, *5*, 258.
- 667 37. Charlton, P.; Birrenkott, D.A.; Bonnici, T.; Pimentel, M.A.; Johnson, A.E.; Alastruey, J.; Tarassenko, L.;
668 Watkinson, P.J.; Beale, R.; Clifton, D.A. Breathing Rate Estimation from the Electrocardiogram and
669 Photoplethysmogram: A Review, 2017.
- 670 38. Millasseau, S.C.; Guigui, F.G.; Kelly, R.P.; Prasad, K.; Cockcroft, J.R.; Ritter, J.M.; Chowienczyk, P.J.
671 Noninvasive assessment of the digital volume pulse: comparison with the peripheral pressure pulse.
672 *Hypertension* **2000**, *36*, 952–956.
- 673 39. Fernandez Tellez, H.; Pattyn, N.; Mairesse, O.; Dolenc-Groselj, L.; Eiken, O.; Mekjavic, I.B.; Migeotte, P.F.;
674 Macdonald-Nethercott, E.; Meeusen, R.; Neyt, X. eAMI: a qualitative quantification of periodic breathing
675 based on amplitude of oscillations. *Sleep* **2015**, *38*, 381–389.
- 676 40. Elgendi, M.; Norton, I.; Brearley, M.; Abbott, D.; Schuurmans, D. Detection of a and b waves in the
677 acceleration photoplethysmogram. *BioMedical Engineering Online* **2014**.
- 678 41. Elgendi, M. Detection of c, d, and e waves in the acceleration photoplethysmogram. *Computer methods and
679 programs in biomedicine* **2014**, *117*, 125–136.
- 680 42. Powell, G.; Percival, I. A spectral entropy method for distinguishing regular and irregular motion of
681 Hamiltonian systems. *Journal of Physics A: Mathematical and General* **1979**, *12*, 2053.
- 682 43. Huang, C.M.; Wei, C.C.; Liao, Y.T.; Chang, H.C.; Kao, S.T.; Li, T.C. Developing the effective method of
683 spectral harmonic energy ratio to analyze the arterial pulse spectrum. *Evidence-Based Complementary and
684 Alternative Medicine* **2011**, 2011.
- 685 44. Tang, A.C.; Chung, J.W.Y.; Wong, T. K. S. Digitalizing Traditional Chinese Medicine Pulse Diagnosis with
686 Artificial Neural Network *Telemedicine and E-Health*, **2012**, *18* 446–453.
- 687 45. Allen, J. Photoplethysmography and its application in clinical physiological measurement. *Physiol Meas*
688 **2007**, *28*, 1–39.

- 689 46. Renevey, P.; Vetter, R.; Krauss, J.; Celka, P.; Depeursinge, Y. Wrist-Located Pulse Detection using (IR)
690 Signals, Activity and Nonlinear Artifact Cancellation. *Proceedings of IEEE EMBS 2001* **2001**, pp. 1–4.
- 691 47. Celka, P.; Vetter, R.; Renevey, P.; Verjus, C.; Neuman, V. Wearable biosensing: signal processing and
692 communication architecture issues. *Journal of Telecommunications and Information Technology, Special Issue on*
693 *e-Health: Wearable devices, Personal Health Management Systems and Services based on biosensors* **2005**, *4*, 90–104.
- 694 48. Celka, P.; Vetter, R.; Gysels, E.; Hine, T. Dealing with randomness in biosignals. In *Winterhalder M; Schelter,*
695 *B.; Timmer, J., Eds.; Wiley-CVH Verlag GmbH & Co, Berlin: Handbook of Time Series Analysis. Recent*
696 *Theoretical Developments and Applications*, 2006; pp. 101–141.
- 697 49. Vetter, R.; Vesin, J.M.; Celka, P.; Renevey, P.; Krauss, J. Automatic Nonlinear Noise Reduction Using Local
698 Component Analysis and {MDL} Parameter Selection. *EMBS 2003, Cancun, Mexico* **2003**, *1*, 491–496.
- 699 50. Cutmore, T.; Celka, P. Composite noise reduction of ERps using wavelets, model-based and principal
700 component analysis subspace methods. *J of Psychophysiology* **2008**, *22*, 111–120.
- 701 51. Mallat, S. *A Wavelet Tour of Signal Processing*; Academic Press, 1998.
- 702 52. Kroenke, K.; Spitzer, R.L. The PHQ-9: A New Depression Diagnostic and Severity Measure. *Psychiatric*
703 *Annals* **2002**, *32*, 509–515.
- 704 53. Scarpina, F.; Tagini, S. The stroop color and word test, **2017**, *8*, 557.
- 705 54. Brook, R.D.; Appel, L.J.; Rubenfire, M.; Ogedegbe, G.; Bisognano, J.D.; Elliott, W.J.; Fuchs, F.D.; Hughes,
706 J.W.; Lackland, D.T.; Staffileno, B.A.; Townsend, R.R.; Rajagopalan, S. Beyond medications and diet:
707 Alternative approaches to lowering blood pressure: A scientific statement from the american heart
708 association. *Hypertension* **2013**.
- 709 55. McCormack, H.M.; Horne, D.J.; Sheather, S. Clinical applications of visual analogue scales: a critical review.
710 *Psychological medicine* **1988**.
- 711 56. Saul, J.; Kaplan, D.; Kitney, R. Nonlinear interactions between respiration and heart rate: a phenomenon
712 common to multiple physiologic states. *Comp. Cardiol.* **1988**, *15*, 12–23.
- 713 57. Arberet, S.; Mathieu, L.; Renevey, P.; Sola, J.; Grossenbacher, O.; Andries, D.; Sartori, C.; Bertschi M.
714 Photoplethysmography-based ambulatory heartbeat monitoring embedded into a dedicated bracelet *IEEE*
715 *Conference, Computing in Cardiology*, **2013**, *40* 935–938.
- 716 58. Lippman, N.; Stein, K.M.; Lerman, B.B. Comparison of methods for removal of ectopy in measurement of
717 heart rate variability. *American Journal of Physiology-Heart and Circulatory Physiology* **1994**, *267*, H411–H418.
- 718 59. Moraes, J.; Rocha, M.; Vasconcelos, G.; Vasconcelos Filho, J.; de Albuquerque, V. Advances in
719 photoplethysmography signal analysis for biomedical applications. *Sensors* **2018**, *18*, 1894.
- 720 60. Wang, Y.; Chang, S.; Wu, Y.; Hsu, T.; Wang, W. Resonance. The missing phenomenon in hemodynamics.
721 *Circulation research* **1991**, *69*, 246–249.
- 722 61. Wang, Y.Y.L.; Hsu, T.L.; Jan, M.Y.; Wang, W.K. Theory and applications of the harmonic analysis of arterial
723 pressure pulse waves. *Journal of Medical and Biological Engineering* **2010**, *30*, 125–131.
- 724 62. Wang, Y.Y.L.; Jan, M.Y.; Shyu, C.S.; Chiang, C.A.; Wang, W.K. The natural frequencies of the arterial system
725 and their relation to the heart rate. *IEEE Transactions on Biomedical Engineering* **2004**, *51*, 193–195.
- 726 63. Chang, C.W.; Liao, K.m.; Chang, Y.T.; Wang, S.H.; Chen, Y.c.; Wang, G.C. The First Harmonic of Radial
727 Pulse as an Early Predictor of Silent Coronary Artery Disease and Adverse Cardiac Events in Type 2
728 Diabetic Patients. *Cardiology research and practice* **2018**, *2018*.
- 729 64. Peng, H.; Long, F.; Ding, C. Feature selection based on mutual information: Criteria of max-dependency,
730 max-relevance, and min-redundancy. *IEEE Trans on Pattern Analysis and Machine Intelligence* **2005**,
731 *27*, 1226–1238.
- 732 65. Schreiber, T.; Schmitz, A. Surrogate time series. *Physica D* **2000**, *142*, 346–382.
- 733 66. Menneer, T. Quantum Artificial Neural Networks. PhD thesis, Faculty of Science, University of Exeter,
734 1998.
- 735 67. Youden, W.J. Index for rating diagnostic tests *Cancer* **2009**, *3*, 32–35.
- 736 68. Wang, L.; Pickwell-Macpherson, E.; Liang, Y.P.; Zhang, Y.T. Noninvasive cardiac output estimation using
737 a novel photoplethysmogram index. *Conference proceedings : Annual International Conference of the IEEE*
738 *Engineering in Medicine and Biology Society. IEEE Engineering in Medicine and Biology Society. Conference* **2009**.
- 739 69. Alty, S. R.; Angarita-Jaimes, N.; Millasseau, S. C.; Chowienczyk, P. J. Predicting arterial stiffness from the
740 digital volume pulse waveform *IEEE Transactions on Biomedical Engineering*, **2007**, *54* 2268–2275.

- 741 70. Sheng, C. S.; Li, Y.; Huang, Q. F.; Kang, Y. Y.; Li, F. K.; Wang, J. G. Pulse Waves in the Lower Extremities as
742 a Diagnostic Tool of Peripheral Arterial Disease and Predictor of Mortality in Elderly Chinese *Hypertension*,
743 **2016**, *18* 527–534.
- 744 71. Hsu, P. C.; Wu, H. T.; Sun, C. K. Assessment of Subtle Changes in Diabetes-Associated Arteriosclerosis
745 using Photoplethysmographic Pulse Wave from Index Finger *Journal of Medical Systems*, **2018**, *42* 43.
- 746 72. Wu, H. T.; Liu, C. C.; Lin, P. H.; Chung, H. M.; Liu, M. C.; Yip, H. K.; Liu, A. B.; Sun, C. K. Novel application
747 of parameters in waveform contour analysis for assessing arterial stiffness in aged and atherosclerotic
748 subjects *Atherosclerosis*, **2010**, *213* 173–177.
- 749 73. Khoury, B.; Sharma, M.; Rush, S.E.; Fournier, C. Mindfulness-based stress reduction for healthy individuals:
750 A meta-analysis, 2015.